

On the Electronic Nature of a Butadienyl Biradical – Experiments and ab initio MO Calculations

Rolf Gleiter*, Hagen Weigl, and Gebhard Haberhauer

Organisch-Chemisches Institut der Universität Heidelberg,
Im Neuenheimer Feld 270, D-69120 Heidelberg, Germany

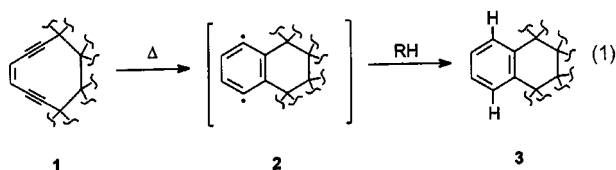
Received March 4, 1998

Keywords: Alkynes / Ab initio calculations / Radicals / Isotope effects

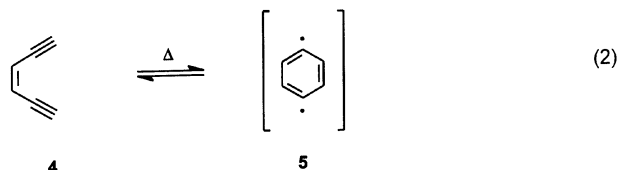
The spin state of the biradical obtained upon heating 1,6-diisopropyl-1,6-diazacyclodeca-3,8-diyne (**9b**) has been investigated. **9b** was heated in biphenyl, naphthalene, and bromobenzene at 150 °C in the presence of a mixture of [D₄]- and [D₀]-9,10-dihydroanthracene (DHA) as hydrogen source. The relative contributions of the cage (C) and cage-escape (E) reaction paths could be determined by analysing the products 2,6-diisopropyl-1,2,3,5,6,7-hexahydro-2,6-naphthyridine (**11b**) and 2,6-diisopropyl-4-(9,10-dihydroanthracenyl)-1,2,3,5,6,7-hexahydro-2,6-naphthyridine (**12b**) and their deuterated analogues. The C/E ratio could be determined by GC-MS analysis and was found to be 0.30 in biphenyl, 0.40 in naphthalene, and 0.22 in bromobenzene,

and to be more or less independent of the DHA concentration over a wide range. The energetics of the cyclization of 1,6-diazacyclodeca-3,8-diyne (**9a**) to 1,2,3,5,6,7-hexahydro-2,6-naphthyridine-2,6-diyl (**10b**) have been investigated at several levels of theory. Calculations of the various structures along the reaction coordinate at the CASPT2/6-31G* level yield an energy difference of 10.7 kcal/mol between **9a** and **10a** and of 17.8 kcal/mol between **9a** and the transition state (**14a**). The transition state shows only weak biradical character, indicating that the electronic structure of **9a** is retained as long as possible. The energy difference between the ¹A_g and ³A_u states of **10a** is predicted to be 13.0 kcal/mol.

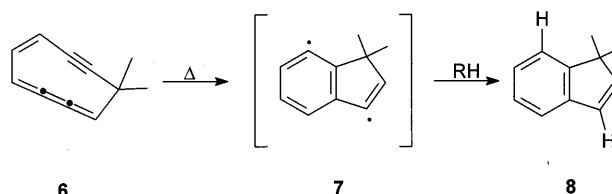
During the last few years, several natural products have been discovered that show antitumor properties.^[1] The molecules that have been studied in most detail are calicheamicin, esperamicin, dynemicin, and neocarcinostatin.^[1] Common to all of them is that their mechanism of action involves a 1,4-biradical, which is formed by a chemical activation step.^{[2][3][4][5]} In the case of the first three of the above antitumor agents, a (Z)-enediyne unit (**1**) in a ten-membered ring reacts to give a 1,4-dehydrobenzene derivative (**2**). In the early 1970s, Bergman and co-workers carried out extensive studies of this ring-closure reaction in hexa-1,5-diyne-3-ene (**4**) and simple derivatives.^[6] Trapping experiments with 1,4-cyclohexadiene indicated a singlet state for the biradical intermediate (**5**).^[7] Gas-phase studies by Roth et al.^[8] led to an activation energy of 28.2 kcal/mol for the conversion of **4** to **5**, and an energy difference between **4** and **5** of 8.5 kcal/mol. Results of sophisticated ab initio calculations^{[9][10]} on the reaction path for the Bergman cyclization of **4** to **5** are in good agreement with these experimental values, and show that the transition state has little biradical character.



In neocarcinostatin, a (Z)-annulenyne system **6** is believed to undergo ring closure. This reaction has recently



been studied by Myers and co-workers using (Z)-1,2,4-heptatrien-6-yne as a model system.^[11]

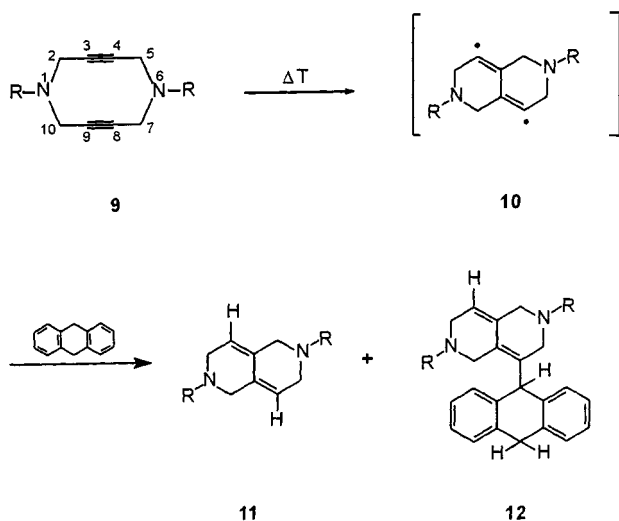


A common feature of both types of cyclization is that a σ 1,4-biradical and the π system of a benzene ring are formed simultaneously. In both precursors, two “in-plane” π bonds are held in close proximity in a medium-sized ring, which form a σ bond and generate two radical centers.

We have recently synthesized a number of cyclic diynes in which two triple bonds are arranged parallel to each other and in close proximity.^[12] In the case of 1,6-diazacyclodeca-3,8-diyne (**9a**) and its 1,6-dialkyl or diaryl congeners, the transannular distance between the triple bonds varies between 2.92 Å and 3.00 Å,^[13] values for which a low activation energy for the Bergman cyclization was predicted. Indeed, upon heating of **9b** at 150 °C in the presence of a hydrogen-atom donor such as 9,10-dihydroanthracene

(DHA), we observed a quantitative reductive cyclization of **9b** to **11b** and **12b**. We rationalized this result by assuming 1,4-biradical **10b** to be an intermediate.^[14]

Scheme 1. R = H(a), *i*Pr (b)



To learn more about the nature of **10**, especially its spin state, we have now carried out chemical trapping experiments and have performed *ab initio* calculations.

Chemical Trapping Experiments

Our experimental studies are based on the assumptions that the biradical **10** abstracts a hydrogen (deuterium) atom from a hydrogen (deuterium) donor, that the spin state of **10** is maintained in the resulting radical pair, and that the reactivity of this radical pair depends on its spin state.^[7] In the case of a triplet radical pair, cage (C) reaction is prohibited by spin, so that the cage-escape reaction (E) occurs. A singlet radical pair may undergo both cage and escape reactions. In order to determine whether singlet and/or triplet radical pairs are formed when **10** is trapped by a hydrogen donor, we have to use the distribution of the products to distinguish between cage and cage-escape reactions. The ratio of the cage to cage-escape reactions (C/E) should tell us about the spin state of the biradical **10** that gives rise to these products.

In Scheme 2 we have illustrated the cage and cage-escape reactions that can occur if the biradical **10b** is generated from **9b** and hydrogen is transferred from a hydrogen donor. We expect two kinds of products, the reduction product **11b** and the recombination product **12b**. Both products may be produced either by cage or cage-escape reactions, and it is necessary to determine to what extent each path contributes to the formation of **11b** and **12b**. Consider the above reaction to be carried out in a 1:1 mixture of 9,10-dihydroantirane ([D₀]DHA) and the corresponding 9,9,10,10-tetra-deutero derivative ([D₄]DHA). The reaction of biradical **10b** with [D₀]DHA will produce the radical [D₀]-**13b**, which may abstract another hydrogen from the radical formed from [D₀]DHA to give [D₀]-**11b**. Alternatively, [D₀]-**13b** may abstract a deuterium from [D₄]DHA to give [D₁]-**11b**, or it

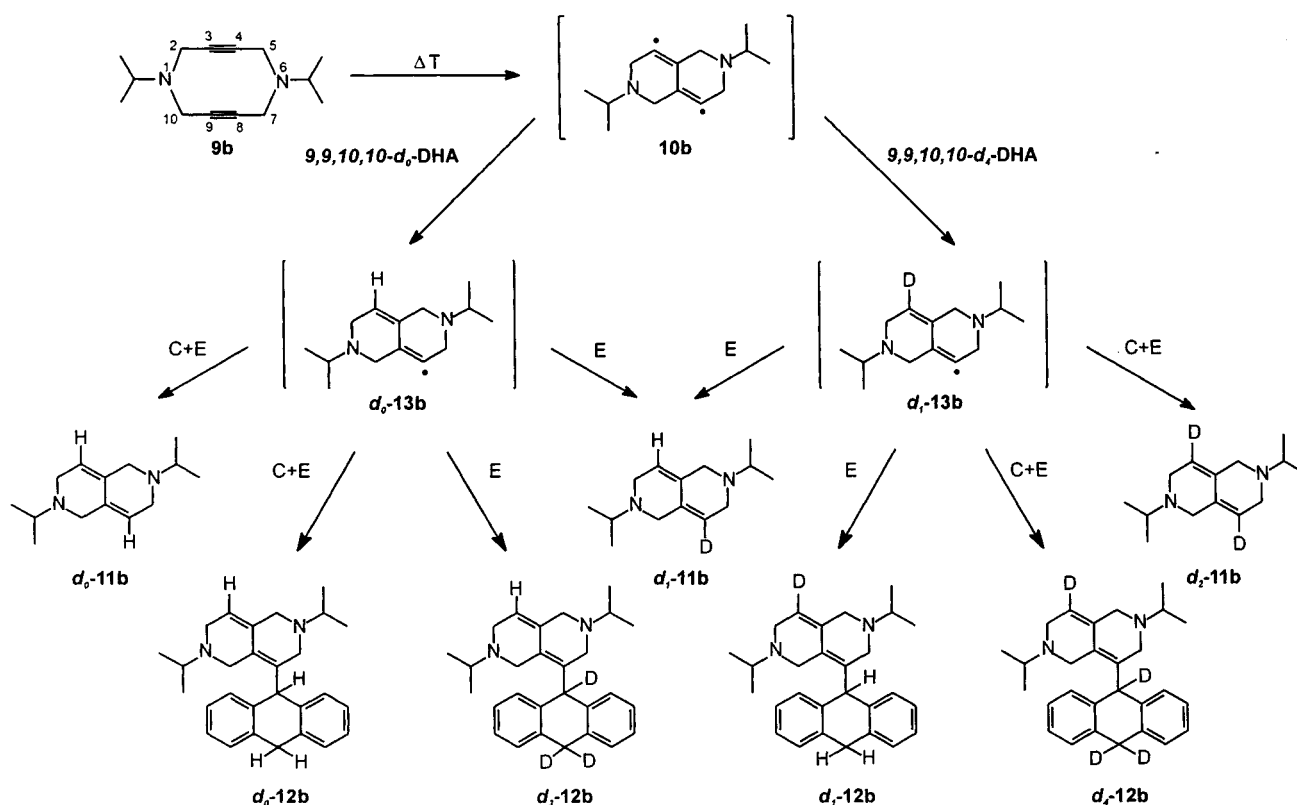
may recombine with the radical generated from either [D₀]DHA or [D₄]DHA to yield [D₀]-**12b** or [D₃]-**12b**, respectively. Escape of [D₀]-**13b** from the solvent cage, followed by abstraction of a hydrogen/deuterium atom from either [D₀]DHA or [D₄]DHA will, in the absence of a deuterium isotope effect, produce [D₀]-**11b** and [D₁]-**11b** in a 1:1 ratio. Similarly, [D₁]-**13b** can undergo an escape reaction to form [D₁]-**11b** or the recombination product [D₁]-**12b**, or it can take part in cage or cage-escape reactions to form [D₂]-**11b** and [D₄]-**12b**, respectively. Cage reactions will produce only [D₀]-**11b**, [D₀]-**12b**, [D₂]-**11b**, and [D₄]-**12b**, while the cage-escape path will additionally lead to [D₁]-**11b**, [D₃]-**12b**, and [D₁]-**12b**. The product [D₂]-**12b** should not be formed.

From these considerations it is clear that, in the absence of isotope effects, from the reaction of **10b** with 1:1 [D₀]DHA and [D₄]DHA, the ratio of [D₀]-**11b**: [D₁]-**11b**: [D₂]-**11b** produced by cage-escape reaction will be 1:2:1. Because [D₁]-**11b** can only be produced by a cage-escape reaction path, from the measured deviation of the [D₀]-, [D₁]-, [D₂]-**11b** ratio from 1:2:1, it is possible to deduce the relative contributions of the cage and cage-escape pathways. Moreover, we expect only the [D₀] and [D₄] recombination products to be formed. A cage-escape reaction leading to [D₀]-, [D₁]-, [D₃]- and [D₄]-**12b** is possible, but not very likely considering the very low concentrations of the two radical species that must combine. Cage recombination within a radical pair can lead only to [D₀]- and [D₄]-**12b**.

In our experiments, we heated **9b** in either biphenyl (in most cases), or in naphthalene, or in bromobenzene at 150°C for 180 minutes. The concentration of DHA was varied from 0.1 mol/l to 1 mol/l. The products were separated from the solvents by extracting the reaction mixture with dilute hydrochloric acid. After neutralization (pH ≈ 9) of the aqueous phase, the organic products were extracted with diethyl ether and were analysed by GC-MS. The peaks for **11b** and **12b** were averaged over the whole widths, to allow for the isotopomeric separation. This was necessary because during the GC-MS analysis the isotopomers of the substances are separated slightly in the course of their passage through the column. As a result, somewhat broadened peaks appear. MS analysis shows that the labelled isotopomers are enriched in the ascendant branch of the peak, whereas the isotopomers with lower mass are concentrated in the decay branch.

In order to determine the kinetic isotope effect, we focussed on the isotopic ratios in **12b**, formed by reaction of **10b** with a 1:1 mixture of [D₄]DHA and [D₀]DHA. We obtained 76% of [D₀]-**12b**, 1% of [D₁]-**12b**, 0% of [D₂]-**12b**, 4% of [D₃]-**12b**, and 19% of [D₄]-**12b** (±1) using a sample of pure [D₀]-**12b** as a reference for the calculation of the isotopomeric distribution (*vide infra*). The amounts of [D₁]- and [D₂]-**12b** are zero within the accuracy of our measurements. The non-zero amount of the [D₃] product is due to the fact that the [D₄]DHA contains some 8% of [D₃]DHA. These results lead to the conclusion that almost all recombination takes place within the solvent cage, as anticipated. The ratio [D₀]-**12b**/[D₄]-**12b** = 4:1 is equal to the kinetic

Scheme 2



isotope effect, which is of the magnitude expected for a primary isotope effect at 150 °C.

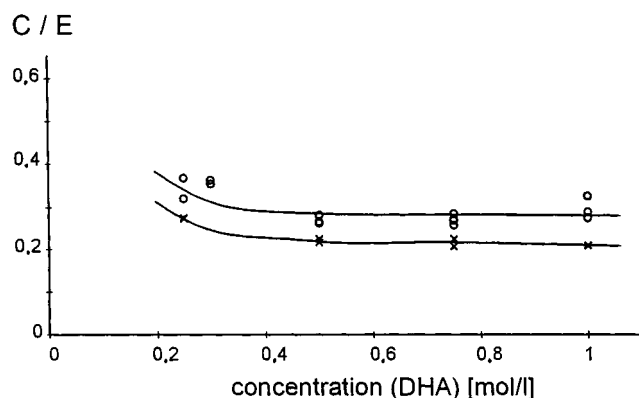
Assuming that the k_H/k_D for the second hydrogen abstraction in forming **11b** is the same as k_H/k_D for the first one, our investigations of the isotopic ratios in **11b**, which give the C/E ratio, were carried out in a solvent containing a mixture of 20% of $[D_0]$ DHA and 80% of $[D_4]$ DHA. The four-fold excess of $[D_4]$ DHA thus cancels the kinetic isotope effect of four. In Figure 1, we show the C/E ratio for product **11b** when **9b** (5 mmol/l) was heated in biphenyl and bromobenzene as solvents, with varying concentrations of DHA.

GC-MS analysis of the products leads to a characteristic pattern around the molecule ion peaks of the isotopomers. Conducting the experiment with pure $[D_0]$ DHA leads to a pattern that reflects the ionization processes in the ion source (i.e. the relative amount of $[M - 1]^{+\bullet}$, $[M]^{+\bullet}$ and $[M + 1]^{+\bullet}$), as well as the natural abundance of isotopes, mainly ^{13}C . This pattern does not include any additional signals due to labelling. With these values it is possible to establish a set of universal parameters for the $[D_0]$ isotopomer. Assuming that the labelled isotopomers behave analogously, it is possible to estimate the relative amounts of the isotopomers from a more complex pattern, such as that which is found using a mixture of $[D_0]$ - and $[D_4]$ DHA. In order to confirm the validity of this procedure, pure $[D_4]$ DHA with known deuterium content was used and the amount of $[D_3]$ -**12b** was indeed as high as expected con-

sidering the isotopic purity of the $[D_4]$ DHA. Using $[D_0]$ - and $[D_4]$ DHA in a ratio of 1:4, so as to neglect the kinetic isotope effect, with subsequent manipulation of the raw data as described, leads to the relative amounts of the product isotopomers, $[D_0]$ -, $[D_1]$ -, and $[D_2]$ -**11b**. $[D_1]$ -**11b** can only be formed following a cage-escape reaction pathway. The probability of formation of $[D_1]$ -**11b** is twice that of the formation of either $[D_0]$ -**11b** or $[D_2]$ -**11b** in a cage-escape reaction. To evaluate the amount of $[D_0]$ - or $[D_2]$ -**11b** formed by cage reaction, it is necessary to subtract half of the amount of $[D_1]$ -**11b**. The quotient of the sum of the differences, i.e. the amount of $[D_0]$ - and $[D_2]$ -**11b** formed in a cage reaction and the sum of the $[D_1]$ -**11b** and the remaining amount of $[D_0]$ - and $[D_2]$ -**11b**, which equals twice the amount of $[D_1]$ -**11b**, gives the cage/cage-escape ratio (C/E).

It is seen that C/E remains nearly constant at DHA concentrations higher than 0.5 mol/l. At lower values, the C/E ratio increases due to an increased reaction of the radical and/or diradical intermediates with the solvent, which increases the amount of $[D_0]$ -**11b** in the product. Since it is mainly the amount of $[D_0]$ -**11b** that is affected by these reactions with the solvent, it is possible to estimate a lower limit for the C/E ratio from the $[D_1]$ to $[D_2]$ ratio. The amount of $[D_1]$ -**11b** may also be artificially enhanced by reactions with the solvent, which makes the apparent C/E ratio a lower limit to the actual one. This limit is found to be 0.25 ± 0.05 .

Figure 1. Ratio of cage to cage-escape products (C/E) observed in the reaction of **9b** (5 mmol/l) in biphenyl (circles) and bromobenzene (crosses) as a function of the concentration of 9,10-dihydroanthracene (DHA; $[D_4]DHA/[D_0]DHA = 4:1$); to guide the eye we have drawn a hyperbolic fit through the data points



The average values of C/E for **11b** are 0.30 ± 0.05 in biphenyl, 0.40 ± 0.05 in naphthalene, and 0.22 ± 0.05 in bromobenzene (see Figure 1). In the absence of a solvent, i.e. in neat DHA, a value of 0.23 ± 0.05 was obtained. The lower value obtained in bromobenzene might be explained by assuming an increase of the intersystem crossing rate of the singlet state of **10b** to its triplet state and, therefore, supports the assumption that the biradical is initially in a singlet state. Such an increase of the intersystem crossing rate in the presence of solvents containing heavy atoms is known from excited state chemistry (heavy atom effect).^[15] However, the differences between the values obtained for the reactions in biphenyl, naphthalene and bromobenzene are too small to be conclusive.

The values obtained from our measurements on **10b** compare well with those obtained by Lockhart and Bergman for dehydrobenzenes.^[7] The reaction carried out for (*Z*)-4,5-diethynyl-4-octene gave a C/E ratio of 0.6 over *all* products, including the recombination products, for which only cage reactions are expected. The C/E ratio was found to be independent of the trapping agent (1,4-cyclohexadiene) concentration, while in bromobenzene the ratio dropped to 0.20.^[7]

Molecular Orbital Calculations

To investigate the electronic structure of **10a** and to compute the activation energy for the transformation **9a** \rightarrow **10a**, we have carried out molecular orbital (MO) calculations. The chair conformation **9a**, with the hydrogen atoms at the nitrogen centers in the axial positions, proved to be the energy minimum in all calculations, and is in fact the confor-

mation found in the solid state.^[13] For the diradical species **10a**, we assumed a half-chair conformation of the six-membered rings, with the NH bonds again in the axial positions. Furthermore, we assumed that the point group C_i is maintained in the transition state (**14a**) for the reaction from **9a** to **10a**.

Reactant **9a** and intermediate **10a** have different types of electronic structures. While **9a** is a closed-shell molecule, **10a** is a biradical. Thus, in calculating the reaction path from **9a** to **10a**, a multiconfigurational approach must be used. We chose to perform CASSCF^[16] calculations. In order to include dynamic electron correlation effects, we used a multireference second-order perturbation treatment (CASPT2)^[17] based on the CASSCF reference.

Model I: The geometries of **9a**, **10a** (1A_g and 3A_u) and **14a** were each optimized using the CASSCF(8,8) method.^{[18][19]} For each of these species, the active space contained all of the out-of-plane π and π^* orbitals and, in the case of **9a**, the in-plane π orbitals as well. For **10a** and **14a**, the active space included the newly formed σ and σ^* orbitals ($17a_g$, $20a_u$) and the two non-bonding orbitals ($18a_u$ and $19a_g$). The 6-31G* basis set was used.

Model II: The structural parameters used for **9a** and **10a** (3A_u) were those found with Model I. The geometries of the transition state **14a** and of the local minimum **10a** (1A_g) were found by carrying out single-point CASPT2 calculations at different C_3-C_8 distances, with all other geometrical parameters optimized at the CASSCF level. Around the transition state and the local minimum, the C_3-C_8 distance was changed in increments of 0.025 Å; for **14a**, the maximum energy point was found, while for **10a** the value of the C_3-C_8 distance that minimized the energy was located. All electrons except those in the 1s core orbitals of N and C were correlated.

Results

Electronic Structure: In the course of the reaction from **9a** to **10a**, the two π and two π^* linear combinations in the molecular plane – $17a_g(\pi_+)$, $18a_u(\pi_-)$, $19a_g(\pi_-^*)$ and $20a_u(\pi_+^*)$ – are transformed into the $C(3)-C(8)$ σ ($17a_g$) and the corresponding σ^* orbital ($20a_u$), plus the two non-bonding orbitals, $18a_u$ and $19a_g$. The latter pair are close in energy, with $18a_u$ calculated to be slightly lower in energy (see Figure 2).

If we consider only the two highest occupied MOs shown in Figure 2, we can write the wave function Ψ of **10a** as follows:

$$\Psi = \alpha \cdot | \dots (17a_g)^2(18a_u)^2 > - \beta | \dots (17a_g)^2(19a_g)^2 >$$

Scheme 3

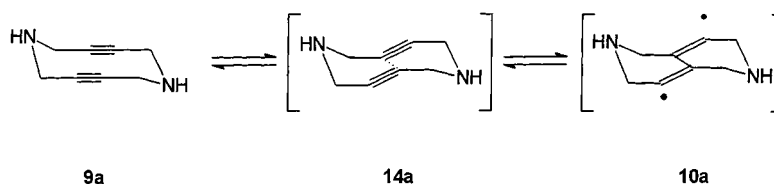
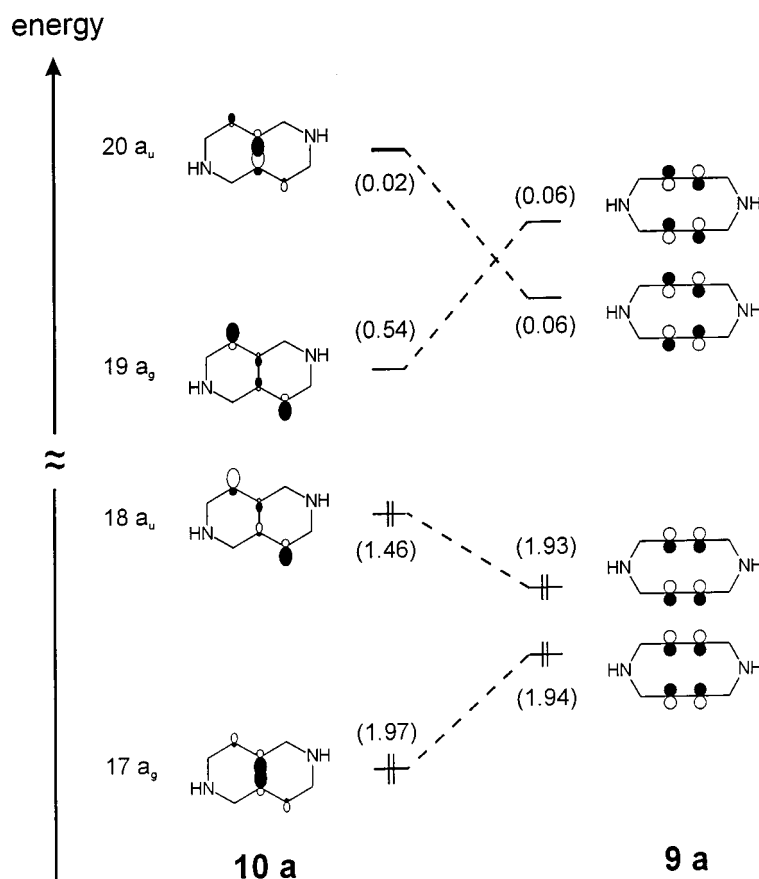


Figure 2. Correlation between the in-plane π -MOs of **9a** with the corresponding MOs of **10a**; the occupation numbers in CASSCF(8,8)/6-31G* of the frontier orbitals are given in brackets



For the electronic configuration of **10a** depicted in Figure 2, β is equal to zero. For a perfect biradical, both frontier orbitals, $18a_u$ and $19a_g$, are equally populated; this amounts to $\alpha^2 + \beta^2 = 1$. The occupation numbers $n(\varphi)$ should be a good measure of the biradical character along the reaction coordinate.

Table 1. Occupation numbers n for the orbitals $18a_u$ and $19a_g$; the values are taken from CASSCF(8,8)/6-31G* calculations

C(3)–C(8) distance		$n(18a_u)$	$n(19a_g)$
3.262	9a	1.930	0.064
2.700		1.924	0.070
2.300		1.905	0.093
2.100	14a	1.879	0.123
1.950		1.825	0.179
1.900		1.793	0.211
1.700	10a	1.599	0.406
1.550		1.459	0.545

In Table 1 we have listed these numbers, while in Figure 2 values are given for **9a** and **10a**. The occupation numbers in Table 1 reveal that the biradical character increases on going from **9a** to **10a**, but that **14a** and **10a** are still far from being genuine biradicals. In contrast to the case of butane-1,3-diyl,^[20] through bond coupling does not become dominant in **10a**. Presumably, this is due to the shorter C–C bond lengths in **10a**, which keep $18a_u$ below $19a_g$.

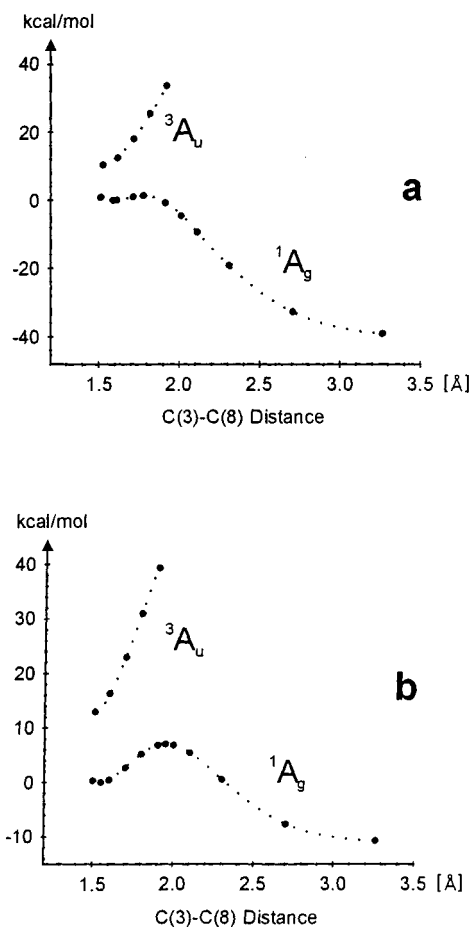
Thermodynamic Data: The energies of **10a** and **14a**, relative to that of **9a**, are given in Table 2 and Figure 3 for each of the different models.

Table 2. Relative energies [kcal/mol] for **9a**, **14a**, and **10a**

	9a	14a	10a
CASSCF(8,8)/6-31G*	0	40.36	39.06
CASPT2/6-31G*	0	17.77	10.68

At the CASPT2N/6-31G* level, we calculate an activation energy of 17.8 kcal/mol for the ring-closure process of **9a** to **10a** and an energy difference of 10.7 kcal/mol between **9a** and **10a**. In the case of 1,6-cyclodecadiyne, we were able to measure the energy difference ΔE between the ground state and the biradical intermediate (24.6 kcal/mol) and the activation energy ($E_a = 28.9$ kcal/mol) in the gas phase.^[21] Using the same level of theory (CASPT2/6-31G*), we found that both values were predicted as being too small ($\Delta E = 14.1$ kcal/mol, $E_a = 21.2$ kcal/mol), but much closer to experiment than the values obtained at the CASSCF(8,8)/6-31G* level.^[22] Therefore, for the values listed in Table 2, we assume that the CASPT2/6-31G* values underestimate the experimental figures by 7–10 kcal/mol, while the CASSCF values deviate by 25 kcal/mol. The differences between calculated (CASPT2) and experimental

Figure 3. Reaction profile of the cyclization **9a** to **10a** with C(3)–C(8) as reaction coordinate, using models I (a) and II (b)



values are due to a systematical error of the used method calculating the heat of reaction and formation of diradicals.^[23] Additionally we have to consider that due to limitation of computational capacities it was impossible to calculate the force constant matrix, so it can not be ruled out, that a lower lying transition state exists, maybe in a lower point group symmetry. We also calculated the triplet energy of **10a**. The values obtained at the different levels of theory are listed in Table 3. It can be seen that at all levels of theory, 1A_g is well below the 3A_u state in energy.

Table 3. Relative energies [kcal/mol] for the 1A_g and 3A_u states of **10a**

Method	1A_g	3A_u
CASSCF(8,8)/6-31G*	0	10.37
CASPT2/6-31G*	0	12.96

Conclusion

Our studies on the thermal cyclization of 1,6-diazacyclodeca-3,8-diyne reveal several similarities to the Bergman cyclization. The chemical trapping experiments with a mixture of labelled and non-labelled 9,10-dihydroanthracene ($[D_0]DHA/[D_4]DHA = 4:1$), in solvents with and without

heavy atoms, suggest a singlet state for the biradical intermediate.

Calculations on both reactions^{[9][10][22]} indicate a similar reaction profile with a “late” transition state. The degree of biradical character of both transition states is low. The main difference between the two reactions is a deeper energy well for the intermediate biradical in the case of the Bergman cyclization. This can be readily understood, since formation of the 6π aromatic system of **5** provides a far greater driving force than formation of the *trans*-diene π system in **10**.

We are grateful to the *Deutsche Forschungsgemeinschaft*, the *Fonds der Chemischen Industrie*, and the *BASF Aktiengesellschaft*, Ludwigshafen, for financial support.

Experimental Section

General Experimental Data: Details of the NMR-, IR-, and mass spectrometers used have been reported in a recent publication.^[24] GC-MS analyses were performed with a Hewlett-Packard 5890 (GC) and 5972 (MSD) instrument. The solvents used for the trapping experiments were biphenyl (Riedel-de Haen), naphthalene (Merck), and bromobenzene. Biphenyl was used as received, naphthalene was purified by sublimation, and bromobenzene was distilled twice in vacuo prior to use. $[D_0]$ Dihydroanthracene (DHA, Aldrich) was recrystallized twice from ethanol before use. All reactions were carried out in dry solvents under argon.

$[D_4]$ Dihydroanthracene: A suspension of 800 mg of oil-free sodium hydride in 30 ml of $[D_6]$ DMSO was heated to 90°C for 90 min. After cooling the solution to 80°C, 15 g (83 mmol) of $[D_0]$ DHA was added, and the mixture was stirred for 30 min. at 80°C. Then, 10 ml of D_2O was added and stirring was continued for 45 min. at 25°C. Subsequently, 40 ml of H_2O was added and the precipitated $[D_4]$ DHA was filtered off, washed with water, and recrystallized from ethanol. To increase the deuterium content of the product it was treated again in the same way to yield 9.27 g (50 mmol) of $[D_4]$ DHA (61%) as colourless needles, m.p. 108–110°C. – 1H NMR (300 MHz, $CDCl_3$): $\delta = 7.33$ (dd, $^3J = 5.5$ Hz, $^3J = 3.5$ Hz, 4 H), 7.24 (dd, $^3J = 5.5$ Hz, $^3J = 3.5$ Hz, 4 H), 3.96 (s, 0.01 H). – ^{13}C NMR (75 MHz, $CDCl_3$): $\delta = 136.85$, 127.60, 126.31; 35.65 (sept, $^1J_{CD} = 20$ Hz). – MS (EI, 8 eV); m/z (%): 180 (1), 182 (1), 183 (8.7) 184 (100).

Thermal Reaction in Biphenyl. – General Procedure (other reactions at different DHA concentrations were conducted using appropriately adjusted quantities of reactants): 90 mg (0.5 mmol) of $[D_0]$ DHA, 368 mg (2.0 mmol) of $[D_4]$ DHA, 5.45 mg (0.025 mmol) of 1,6-diisopropyl-1,6-diazacyclodeca-3,8-diyne (**9b**) and 4.5 g of biphenyl were placed in a 25-ml flask. Oxygen was removed by applying a vacuum and flushing with argon three times. The mixture was then heated to 150°C under argon. After 180 min, a sample (ca. 1 ml) was withdrawn using a pipette, which was diluted with 2 ml of diethyl ether and stirred with 2 ml of 2 N aqueous HCl solution. After phase separation, the acidic phase was treated with 4 ml of 2 N NaOH. Re-extraction of the free amines with 2 ml of diethyl ether and drying of the organic layer ($MgSO_4$) gave a solution of the products which was used for GC-MS analysis without further purification.

GC-MS Analysis of the Trapping Experiments: The experiment was carried out at a dihydroanthracene (DHA) concentration of 0.25 mol/l. Applying only $[D_0]$ DHA gave the following relative abundances around the molecular-ion peak of pure $[D_0]$ -**11b** (the

intensities in parentheses were normalized to 1000 for the highest peak); m/z : 219 $[M - 1]^+ \bullet$ (339), 220 $[M]^+ \bullet$ (1000), 221 $[M + 1]^+ \bullet$ (164). The values for $[M - 2]^+$ and $[M + 2]^+$ were lower than 5% and were therefore neglected. Analysis of a sample obtained by using a 1:4 mixture of $[D_0]$ - and $[D_4]$ DHA (0.25 mol/l) gave the following abundances of the ions; m/z : 220 (1612), 221 (2053), 222 (1421). The abundances were determined by averaging over the whole peak width using the standard routine of the HP-MSD software package. For abundances of the $[M - 1]^+ \bullet$, $[M]^+ \bullet$ and $[M + 1]^+ \bullet$ peaks of the isotopomers of **11b**, the following equations result:

$$[220] = [M]^+ \bullet ([D_0]\text{-}\mathbf{11b}) + [M - 1]^+ \bullet ([D_1]\text{-}\mathbf{11b})$$

$$[221] = [M + 1]^+ \bullet ([D_0]\text{-}\mathbf{11b}) + [M]^+ \bullet ([D_1]\text{-}\mathbf{11b}) + [M - 1]^+ \bullet ([D_2]\text{-}\mathbf{11b})$$

$$[222] = [M + 1]^+ \bullet ([D_1]\text{-}\mathbf{11b}) + [M]^+ \bullet ([D_2]\text{-}\mathbf{11b})$$

Insertion of the above parameters leads to the following set of equations:

$$1652 = 1000 ([D_0]\text{-}\mathbf{11b}) + 339 ([D_1]\text{-}\mathbf{11b})$$

$$2053 = 164 ([D_0]\text{-}\mathbf{11b}) + 1000 ([D_1]\text{-}\mathbf{11b}) + 339 ([D_2]\text{-}\mathbf{11b})$$

$$1421 = 164 ([D_1]\text{-}\mathbf{11b}) + 1000 ([D_2]\text{-}\mathbf{11b})$$

Solving this system of equations by standard algebraic methods yields $[D_0]\text{-}\mathbf{11b} = 82.3$, $[D_1]\text{-}\mathbf{11b} = 100$, $[D_2]\text{-}\mathbf{11b} = 81.2$. The C/E ratio is then calculated as:

$$C/E = \{([D_0]\text{-}\mathbf{11b}) - ([D_1]\text{-}\mathbf{11b}) + ([D_2]\text{-}\mathbf{11b})\} / 2 ([D_1]\text{-}\mathbf{11b}) = 0.32$$

The contribution of the isotopomers of **12b** was evaluated in a similar way by also taking into account the $[M - 2]^+ \bullet$ and $[M + 2]^+ \bullet$ peaks. This led to five equations, which were solved analogously.

- [1] Reviews: K. C. Nicolaou, W.-M. Dai, *Angew. Chem.* **1991**, *103*, 1453; *Angew. Chem. Int. Ed. Engl.* **1991**, *30*, 1387; K. C. Nicolaou, A. L. Smith, *Acc. Chem. Res.* **1992**, *25*, 497; K. C. Nicolaou, A. L. Smith, in *Modern Acetylene Chemistry* (Eds.: P. J. Stang, F. Diederich), VCH, Weinheim, **1995**, 203.
- [2] M. D. Lee, T. S. Dunne, M. M. Siegel, C. C. Chang, G. O. Morton, D. B. Borders, *J. Am. Chem. Soc.* **1987**, *109*, 3464; M. D. Lee, T. S. Dunne, C. C. Chang, G. A. Ellestad, M. M. Siegel, G. O. Morton, W. J. McGahren, D. B. Borders, *J. Am. Chem. Soc.* **1987**, *109*, 3466.
- [3] J. Golik, J. Clardy, G. Dubay, G. Groenewold, H. Kawaguchi, M. Konishi, B. Krishnan, H. Ohkuma, K.-I. Saitoh, T. W. Doyle, *J. Am. Chem. Soc.* **1987**, *109*, 3461; J. Golik, G. Dubay, G. Groenewold, H. Kawaguchi, M. Konishi, B. Krishnan, H.

- Ohkuma, K.-I. Saitoh, T. W. Doyle, *J. Am. Chem. Soc.* **1987**, *109*, 3462.
- [4] M. Konishi, H. Ohkuma, T. Tsuno, T. Oki, G. D. van Duyne, J. Clardy, *J. Am. Chem. Soc.* **1990**, *112*, 3715.
- [5] A. G. Myers, *Tetrahedron Lett.* **1987**, *28*, 4493; A. G. Myers, P. J. Proteau, T. M. Handel, *J. Am. Chem. Soc.* **1988**, *110*, 7212; A. G. Myers, P. J. Proteau, *J. Am. Chem. Soc.* **1989**, *111*, 1146.
- [6] R. G. Bergman, *Acc. Chem. Res.* **1973**, *6*, 25; R. R. Jones, R. G. Bergman, *J. Am. Chem. Soc.* **1972**, *94*, 660.
- [7] T. P. Lockhart, A. G. Bergman, *J. Am. Chem. Soc.* **1981**, *103*, 4091; T. P. Lockhart, P. B. Comita, R. G. Bergman, *J. Am. Chem. Soc.* **1981**, *103*, 4082.
- [8] W. R. Roth, H. Hopf, C. Horn, *Chem. Ber.* **1994**, *127*, 1765.
- [9] R. Lindh, B. J. Persson, *J. Am. Chem. Soc.* **1994**, *116*, 4963.
- [10] E. Kraka, D. Cremer, *J. Am. Chem. Soc.* **1994**, *116*, 4929.
- [11] A. G. Myers, P. S. Dragovich, E. Y. Kuo, *J. Am. Chem. Soc.* **1992**, *114*, 9369.
- [12] R. Gleiter, *Angew. Chem.* **1992**, *104*, 29; *Angew. Chem. Int. Ed. Engl.* **1992**, *31*, 27; R. Gleiter, R. Merger, in *Modern Acetylene Chemistry* (Eds.: P. J. Stang, F. Diederich), VCH, Weinheim, **1995**, 285.
- [13] R. Gleiter, J. Ritter, H. Irngartinger, J. Lichtenthäler, *Tetrahedron Lett.* **1991**, *32*, 2883; R. Gleiter, J. Ritter, H. Irngartinger, T. Oeser, *J. Am. Chem. Soc.* **1997**, *119*, 10599.
- [14] R. Gleiter, J. Ritter, *Angew. Chem.* **1994**, *106*, 2550; *Angew. Chem. Int. Ed. Engl.* **1994**, *33*, 2470.
- [15] D. O. Cowan, R. L. Drisko, *Elements of Organic Photochemistry*, Plenum Press, New York, **1976**.
- [16] B. O. Roos, *Adv. Chem. Phys.* **1987**, *69*, 399; B. O. Roos, *Int. J. Quantum Chem. Symp.* **1980**, *14*, 175.
- [17] K. Andersson, P.-A. Malmquist, B. O. Roos, A. Sadlej, K. Wolinski, *J. Phys. Chem.* **1990**, *94*, 5483; K. Andersson, P.-A. Malmquist, B. O. Roos, *J. Chem. Phys.* **1992**, *96*, 1218.
- [18] All CASSCF(8,8) and CASPT2 calculations were carried out using the MOLCAS 3 program: K. Andersson, M. R. A. Blomberg, M. P. Fülscher, G. Karlström, V. Kellö, R. Lindh, P.-A. Malmqvist, J. Noga, J. Olsen, B. O. Roos, A. J. Sadlej, P. E. M. Siegbahn, M. Urban, P.-O. Widmark, MOLCAS, University of Lund, **1994**.
- [19] 6-31G* basis set: R. Ditchfield, W. J. Hehre, J. A. Pople, *J. Chem. Phys.* **1971**, *54*, 724; W. J. Hehre, R. Ditchfield, J. A. Pople, *J. Chem. Phys.* **1972**, *56*, 2257; P. C. Hariharan, J. A. Pople, *Theor. Chim. Acta* **1973**, *28*, 213; P. C. Hariharan, J. A. Pople, *Mol. Phys.* **1974**, *27*, 209; M. S. Gordon, *Chem. Phys. Lett.* **1980**, *76*, 163.
- [20] R. Hoffmann, S. Swaminathan, B. G. Odell, R. Gleiter, *J. Am. Chem. Soc.* **1970**, *92*, 7091; P. Du, W. T. Borden, *ibid.* **1987**, *109*, 930; P. Nachtigall, K. D. Jordan, *ibid.* **1992**, *114*, 4743; **1993**, *115*, 270.
- [21] W. R. Roth, T. Wasser, R. Gleiter, H. Weigl, *Liebigs Ann.* **1997**, 1329.
- [22] G. Haberhauer, R. Gleiter, to be published.
- [23] K. Andersson, B. O. Roos, *Int. J. Quantum Chem.* **1993**, *45*, 591.
- [24] F. Ohlbach, R. Gleiter, T. Oeser, H. Irngartinger, *Liebigs Ann.* **1996**, 791.

[98079]